AIAA 81-0235R

Pulsed Doppler Radar Detects Weather Hazards to Aviation

D. S. Zrnic'* and J. T. Lee†
National Severe Storms Laboratory, NOAA, Norman, Okla.

Over the last several years experiments were conducted with a pulsed Doppler radar that have significant consequences for hazard detection in the en route and terminal areas. Mesocyclones can be detected to over 250 km while tornadoes are seen to about 150 km. The radar can detect strong straight winds if they have a significant component along the beam. It is definitely demonstrated that aircraft measured turbulence correlates with the spread of the Doppler spectrum, but caution must be exercised in interpreting the Doppler spectrum width data because these are more prone to gross errors due to noise, antenna sidelobes, ground clutter, etc. Measurements of transient wind phenomena associated with thunderstorms near the airport require a suitably located radar, but it is not yet clear whether these can be always recognized. It appears that monitoring of winds along an aircraft glide path in clear air or otherwise is feasible.

I. Introduction

PRESENTLY three government organizations, the National Oceanic and Atmospheric Administration (NOAA), the Air Force Weather Service (AWS), and the Federal Aviation Administration (FAA) are contemplating deployment and joint use of pulse Doppler radars. Of particular interest to aviation are the detection and monitoring of weather hazards for aircraft en route and in the terminal area. Experiments by various research groups have demonstrated that the Doppler radar can differentiate between tornadic and nontornadic storms. Limited data to date suggest that turbulent areas in a storm system may be recognized from the measurement of velocity spreads (Doppler spectrum width) in a resolution volume. This, coupled with the capability to measure wind speeds and shear should reduce the false alarm rates and increase the safety factor for aircraft in the vicinity of thunderstorms. Thus valuable air space will not be lost due to overwarning and, at the same time, the comfort and safety of passengers will be increased.

There is no doubt that a Doppler radar can detect hazards on and around airports, but it is less clear what scanning strategies need to be employed, where the radar should be sited, or what sensitivity and resolution it should have.

In this paper some experiments at the National Severe Storms Laboratory (NSSL) that have shown potential usefulness to aviation are discussed. The NSSL Doppler radar has moderate power (peak 1 MW), a pencil beam antenna (beamwidth 0. 8 deg), and a wavelength of 10 cm. This allows high-resolution observation of storms a few hundred kilometers away with little attenuation by precipitation and even permits monitoring of wind in the optically clear planetary boundary layer.

II. The Doppler Concept

The pulsed Doppler radar provides the following three estimates: 1) the echo power or zero moment of the Doppler spectrum (this is an indicator of liquid water content in the resolution volume), 2) the mean Doppler velocity or the first moment of the spectrum normalized to the zeroth moment (this is equal to the mean motion of scatterers, which is essentially the air motion towards or away from the radar), and 3) spectrum width σ_v, the square root of the second moment about the first of the normalized spectrum, a measure of velocity dispersion (i.e., shear or turbulence) within the resolution volume.

The very nature of the weather echo imposes limitations and tradeoffs on the use of Doppler radar. Weather targets are distributed quasicontinuously over large spatial regions (tens to hundreds of kilometers); the strength of significant weather echoes easily spans an 80-dB power range; and the signals themselves are semicoherent, i.e., they are not purely sinusoidal.

The unambiguous range (r_a) is the maximum distance a transmitted pulse can travel out and return echoes to the radar before the next pulse is transmitted. When a precipitation area is located beyond the unambiguous range, the echoes returning from that area arrive after the next pulse is transmitted. Radars having uniform pulse repetition time cannot discriminate between echoes coming from scatterers located at distances which fall within the different annuli (trips) of $r_a = cT_s/2$ (where c = light velocity and T_s = repetition time).

It can be shown that the maximum unambiguous Doppler velocity (v_a) measured by a Doppler radar is $v_a = \pm\lambda/4T_s$, where λ is radar wavelength. A basic dilemma associated with the use of Doppler radars becomes apparent when the unambiguous range and velocity are combined:

$$v_a r_a = \lambda c/8 \tag{1}$$

For the study of severe storms in Oklahoma, large unambiguous velocities and ranges are required. One must then use as long a wavelength as is practical, considering beamwidth and antenna size limitations. Longer wavelength also reduces signal attenuation by heavy precipitation areas in severe storms. At the 10-cm wavelengths, the compromise chosen for the two NSSL Doppler radars in standard operating mode was for a maximum range of 115 km and maximum velocity of ± 35 m s^{-1}.

Fully coherent pulsed Doppler radars (i.e., coherency or phase sensitivity is maintained by the radar for more than one PRT) can measure precisely ranges and velocities of targets beyond the first range ambiguity. Similarly, good estimates of velocities past the ambiguous (Nyquist) velocity are possible. Some methods for achieving this and extending r_a and v_a well above the value given by Eq. (1) are discussed by Doviak et al.[1]

The most severe restriction imposed on the Doppler weather radar comes from the semicoherency of the weather echo signal, i.e., the changing of resultant phase that arises from the motion of individual scattering elements (e.g., raindrops) relative to each other. Signal samples spaced T_s apart must be

Presented as Paper 81-0235 at the AIAA 19th Aerospace Sciences Meeting, St. Louis, Mo., Jan. 12-15, 1981; submitted March 3, 1981; revision received June 16, 1981. This paper is declared a work of the U.S. Government and therefore is in the public domain.

*Leader, Doppler Radar Project, Advanced Techniques Group.
†Meteorologist, Advanced Techniques Group.

correlated for precise Doppler shift measurement. Correlation exists when

$$c/4r_a > 2\pi\sigma_v \tag{2}$$

where σ_v is the velocity spectrum width of echoes at range r.[2] Condition (2) merely states that Doppler width should be much smaller than the Nyquist interval $\lambda/2T_s$. When correlation decreases appreciably, the variance in mean Doppler estimate increases exponentially, as does the variance of spectrum width estimate.[3] Requirement (2) means that σ_v limits the largest unambiguous range for a given wavelength, whereas Eq. (1) restricts r_a only if ambiguities due to velocity aliases need to be resolved by choosing a large v_a.

III. Spectral Moment Estimation

Because moment estimates utilize samples of a randomly varying signal, a large number of echo samples (acquired during a few milliseconds) must be processed to provide the required accuracy. The accuracy of these estimates depends directly on the signal-to-noise ratio, distribution of velocities within the resolution volume, receiver transfer, and number of samples processed. Because samples are collected while the antenna is rotating, the desired precision that determines the collection time (dwell time) also restricts the rotation rate.

To obtain a quantitative estimate of echo power, samples must be averaged over a period long compared to the decorrelation time (reciprocal of Doppler spectrum width). A uniformly weighted average obtained from M complex video samples V_n's is

$$\hat{P} = \frac{1}{M}\sum_{n=1}^{M} |V_n|^2 - N \tag{3}$$

where N is the radar white noise power. V_n's are voltages with magnitude and phase corresponding to the electric field echoes from scatterers.

While both coherent and incoherent radars can be used to estimate the zeroth and the second spectral moment, only the Doppler radar provides the first spectral moment estimate. The autocovariance processor for mean velocity (popularly known as pulse pair) is an excellent example of a blend between theoretical ingenuity (the algorithm) and technological advance (integrated digital circuits). Because the autocovariance $R(T_s)$ and the Doppler spectrum constitute a Fourier transform pair, the moments of the spectral density correspond to the derivatives of the complex autocovariance evaluated at zero lag. The pulse pair velocity estimate $\hat{v}_{pp}$ is defined as

$$\hat{v}_{pp} = (v_a/\pi)\arg[\hat{R}(T_s)] \tag{4}$$

where the autocovariance estimate $\hat{R}(T_s)$ is obtained from video samples V_n's:

$$\hat{R}(T_s) = \frac{1}{M}\sum_{n=1}^{M} V_{n+1}V_n^* \tag{5}$$

and * denotes the complex conjugate.

It can be shown that spectral analysis requires $\log_2 M$ times as many operations as the autocovariance method and in addition needs M times more storage locations. However, only the advent of new digital circuits made it possible to produce low cost and reliable autocovariance processors with speed and accuracy to match the information inherent in the Doppler radar signals. This is because the weather radar must make velocity estimates at a very large number (several hundred) of contiguous range locations and at a rate compatible with radar PRF! Besides its efficiency and modest memory storage, the algorithm is very close to a theoretical optimum, i.e., minimum variance estimator.

Second moment estimators based on Fourier methods and pulse pair processing have proved to be useful. The pulse pair algorithm for spectrum width σ_v reads

$$\sigma_v = (\sqrt{2}v_a/\pi)\sqrt{\ell n[\hat{P}/|\hat{R}(T_s)|]} \tag{6}$$

In order for Eq. (6) to be accurate, the spectrum shape must be nearly Gaussian (which is the case for weather signals) and spurious signals must be kept at a minimum. Although spectrum width can be indicative of turbulence, shear, and vortices, it has not yet been as fully tested as the mean velocity, and is now a focus of research at NSSL, sponsored by the Federal Aviation Administration.[4]

IV. Doppler Spectrum Width Shear and Turbulence

If each of the spectral broadening mechanisms are independent of one another, the total velocity spectrum width σ_v can be considered as a sum of σ^2 contributed by each one.[5] That is,

$$\sigma_v^2 = \sigma_s^2 + \sigma_\alpha^2 + \sigma_d^2 + \sigma_t^2 \tag{7}$$

where σ_s^2 is due to shear, σ_α^2 to antenna rotation, σ_d^2 to different drop size fall speeds,[6] and σ_t^2 to turbulence. The components σ_α^2 and σ_d^2 are related to the radar and meteorological parameters.[7] For elevation angles less than 20 deg and rotation rates under 8 deg s^{-1} both terms are smaller than 0.2 $m^2 s^{-2}$. Thus the main contributors to width are shear and turbulence. The wind shear term is composed of three components, i.e., radial velocity shear along the elevation $\sigma_{s\theta}$, azimuth $\sigma_{s\theta}$, and radial directions σ_{sr}.

$$\sigma_s^2 = \sigma_{s\phi}^2 + \sigma_{s\phi}^2 + \sigma_{sr}^2 \tag{8}$$

The assumptions behind Eq. (8) are that shear is constant within the resolution volume and that the antenna pattern is product separable in the θ, ϕ directions. If k_θ and k_ϕ are shears in the θ, ϕ directions, one can show that their contribution to the spectrum width at a range r is[5]

$$\sigma_{s\theta}^2 + \sigma_{s\phi}^2 = (k_\theta^2 + k_\phi^2)r^2\theta_1^2/16\ell n2 \tag{9}$$

Contributions (9) can be estimated from Doppler velocity measurements in adjacent azimuths and elevations. In most practical situations σ_{sr}^2 is insignificant; for instance, with a shear of 10^{-3} s^{-1}, it is about 0.05 m^2 s^{-2}.[5]

If turbulence is homogeneous and isotropic within the resolution volume, Frisch and Clifford[8] have shown that σ_t^2 is related to eddy dissipation rate ϵ in the following way:

$$\sigma_t^2 = A\Gamma(2/3)(\epsilon r\sigma_\theta)^{2/3} \tag{10}$$

where the gamma function $\Gamma(2/3) = 1.354...$, and $\sigma_\theta^2 = \theta_1^2/16\ell n2$. The antenna pattern is assumed Gaussian and circularly symmetric, and the range extent small compared to beamwidth θ_1 typical for most weather radar measurements.

Assuming an eddy dissipation rate $\epsilon \simeq 1$ $m^2 s^{-3}$ and a beamwidth $\theta_1 = 1.4\times10^{-2}$ rad (0.8 deg), we find that width due to turbulence of rather large intensity (i.e., $\epsilon = 1$ m^2 s^{-3}) is $\sigma_t = 6$ m s^{-1}. Eddy dissipation rate near this level is often found in severe thunderstorms.[9]

V. Experiments Related to Aviation

Beginning in 1973 a series of experiments were begun using Doppler weather radar to study weather hazards to aviation. These joint experiments involved the United States Air Force (USAF), Federal Aviation Administration (FAA), National Aeronautics and Space Administration (NASA), Colorado State University (CSU), University of Oklahoma (OU), as well as various National Oceanic and Atmospheric Administration (NOAA) components, and use of penetration aircraft such as the F-4-C, F-101, and F-106 suitably equipped

to make in situ wind and turbulence measurements simultaneously with the radar data collection.[10]

Aircraft tracking was accomplished with transponder data fed into the WSR-57 10-cm weather radar system and displayed simultaneously with contours of radar echo reflectivity. This photographed display provides an aircraft position every 20 s. For analysis, straight line interpolation was used between each recorded position. Radio station WWV time signals were used to coordinate aircraft, weather radar, Doppler radar, and voice data. A 1-km-radius circle of error is probable. Aircraft data were recorded at 50 s^{-1} and a five-point smoothed average provided 0.1-s resolution for computation of true vertical velocities (w) and as a measure of turbulence, derived gust velocities (U_{de}).[11] Derived gust velocities can be divided into four categories of turbulence as follows:

light	$=3.0 \leq U_{de} \leq 6.0$ m s^{-1}	(10-19 ft s^{-1})
moderate	$=6.1 \leq U_{de} \leq 9.1$ m s^{-1}	(20-29 ft s^{-1})
severe	$=9.2 \leq U_{de} \leq 12.1$ m s^{-1}	(30-39 ft s^{-1})
extreme	$=U_{de} \geq 12.2$ m s^{-1}	($\geq$40 ft s^{-1})

The aircraft true airspeed was approximately 170 m s^{-1} for the F-100 and F-4-C and 210 m s^{-1} for the F-101. Thus 0.1-s data points correspond to observations about every 20 m.

The Doppler primarily measures the horizontal wind component. With aircraft, the vertical component is also measured. However, studies such as by Ashburn et al.[12] have shown that turbulence affecting aircraft above the boundary layer is mainly isotropic, particularly so in convective clouds.

A. Turbulence

1. Plan Shear Indicator Test

One phase of the experiment involved the Air Force Cambridge Research Laboratory (AFCRL)-developed Plan Shear Indicator (PSI); the device graphically depicts shear (Fig. 1).[13] The Air Force Aeronautical Systems Division's (ASD) 4950th Test Wing operated an instrumented F-100 in support of the program. CSU supplied a similarly equipped F-101.

When a storm with intensity larger than 30 dBZ approached or appeared within the acceptable radar ranges, aircraft were launched and vectored to the storm area avoiding reflectivity zones greater than 50 dBZ where damaging hail is common.[14]

The PSI has a range resolution of 855 m, and the 0.8-deg beamwidth provides an azimuthal resolution of about 1.1 km at 80 km. Hence we are concerned with turbulent encounters of several seconds or more. More specifically, the 0.1-s aircraft data output corresponds to a maximum unambiguous frequency (f_{max}) of 5 Hz and a corresponding minimum wavelength (L_{min}) represented by

$$L_{min} = (V \pm V')(f_{max})^{-1} \tag{11}$$

where V is aircraft speed and V' the wind speed. Assuming the winds are contained within the maximum unambiguous velocity of the Doppler radar ($\pm$34 m s^{-1}) and that the Taylor hypothesis holds, L_{min} is 30-40 m. The maximum wavelength resolvable is equipment dependent and is considered about 1500 m.

In the Doppler data field, L_{min} is dependent on range and aspect angle due to polar grid characteristics. In the series of complete Doppler spectrum data, the sampling interval of 300 m yields L_{min} = 600 m. At the PSI working distance of 60 km, the 0.8-deg beamwidth provides L_{min} of about 1600 m. Data obtained within a pulse volume have contributions from several integrated factors throughout the total volume (i.e., shear, turbulence; see Sec. V. B) which is quite large (3.308×10^8 m^3 at 60 km) and it is difficult to define turbulent wavelengths within the volume. Thereby we see that pattern correspondence, rather than point-to-point correspondence, must be utilized in correlation studies.

The F-101 made penetration on six days; not all data from these flights are available. The F-100 aircraft penetrated thunderstorms on five days. On three of these days (12 penetrations) it was possible to compare PSI presentation and U_{de}.

Moderate or severe turbulence was encountered in all cases when the PSI displayed wiggles along the aircraft flight path, but wiggles were not present with all turbulence encounters. Thus it appears from these cases that turbulence up through moderate ($U_{de} < 9.1$ m s^{-1}) may escape detection by the PSI. This is not surprising since turbulence need not be generated by horizontal shear. Where severe turbulence ($U_{de} > 9.1$ m s^{-1}) repeatedly was encountered, the PSI showed transient shear areas along the flight path. Arc deformations apparently have an operational detectability threshold associated with wind shears $\geq 1.5 \times 10^{-2}$ s^{-1}.

2. Improved Single Doppler Display

Second-generation radar real-time display, necessary in defining the hazardous areas, was developed in 1974 at the NSSL. The three spectral moments are presented in a field of arrows shown by a minicomputer-graphic display terminal

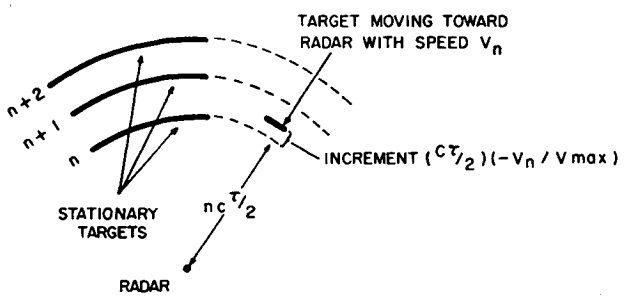

Fig. 1 PSI display for stationary targets (left) and a moving target (right). The moving target is located at the same distance from the radar as the nearest stationary target, but is displaced from it on the PSI display by an increment which depends on its velocity.

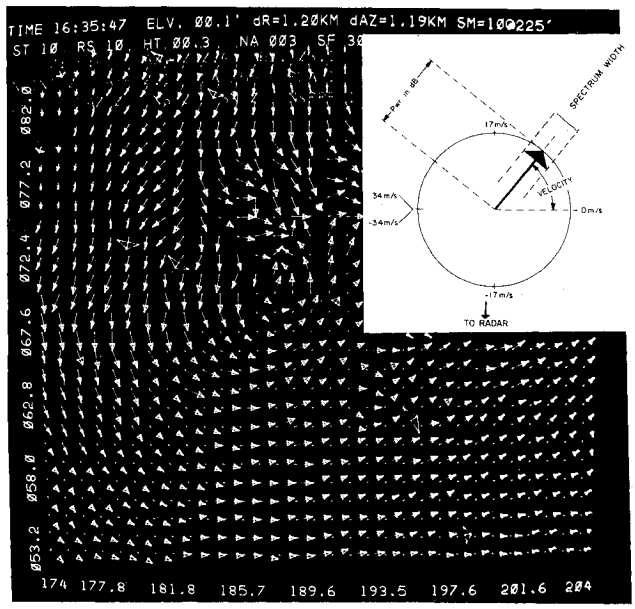

Fig. 2 The multimoment Doppler of a mesocyclone. Each arrow contains information of the three principal Doppler spectrum moments for a resolution volume. For interpretation of arrows see insert in upper right corner (arrow length is proportional to received power, arrow direction to velocity, and arrowhead size to Doppler spectrum width). Abscissa is azimuth and ordinate scale denotes range (km) from radar. Housekeeping information is at top of screen.

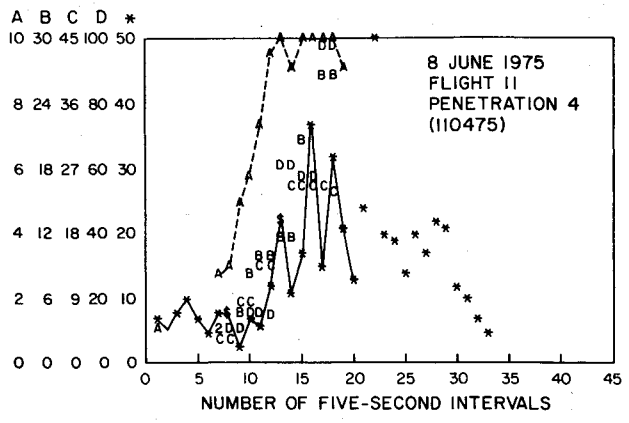

Fig. 3 June 8, 1975, penetration 4: Time (space) profiles of maximum values recorded for each 5 s of flight and corresponding Doppler radar data during penetration. Derived gust velocity: * (ft s^{-1}); spectrum width: A (m s^{-1}); velocity gradient: B (s^{-1} x 1000). D: Laplacian; 2: two data points at the same place. Dashed line connects values of spectrum width and solid line, the derived gust velocities.

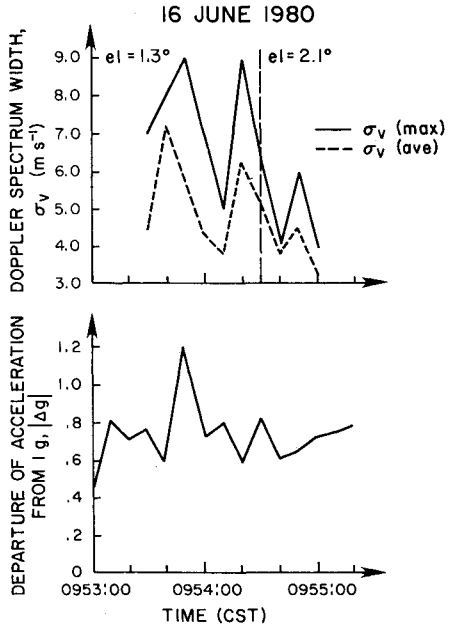

Fig. 4 Doppler spectrum width and the magnitude of vertical aircraft acceleration with respect to 1 *g*. The aircraft speed was near 200 m s^{-1} at an altitude of 4.4 km above ground. Radar data from two elevation angles provide the basis for comparison, 1.3 deg at further range (time less than 0954:30) and 2.1 deg closer in. The crossover occurs at a range where the aircraft to radar line makes a 1.5 deg angle with tangent plane at radar site, which here is also a 3 dB point of the antenna pattern.

interfaced to an NSSL 10-cm Doppler radar.[15] Arrow length is proportional to the log of received power, arrow direction to velocity, and arrowhead size to Doppler spectrum width.

The insert on Fig. 2 illustrates the above relations. Zero velocity is a horizontal arrow pointing right and nonzero velocities are proportional to angular rotation from the zero position (clockwise, negative, i.e., toward the radar, and conversely, counterclockwise, positive). The horizontal arrow pointing left corresponds to the maximum unambiguous velocity (±34 m s^{-1}) resolved by the radar. The display (Fig. 2) is a range vs azimuth presentation of Doppler moments. The display sector can be changed quickly to check large storm regions for wind shear, turbulence, and vortex motion. Note the mesoscale vortex in Fig. 2 at 187 deg and 71 km where we have 20 m s^{-1} winds toward the radar adjacent to 14 m s^{-1} away from the radar—a typical vortex couplet.

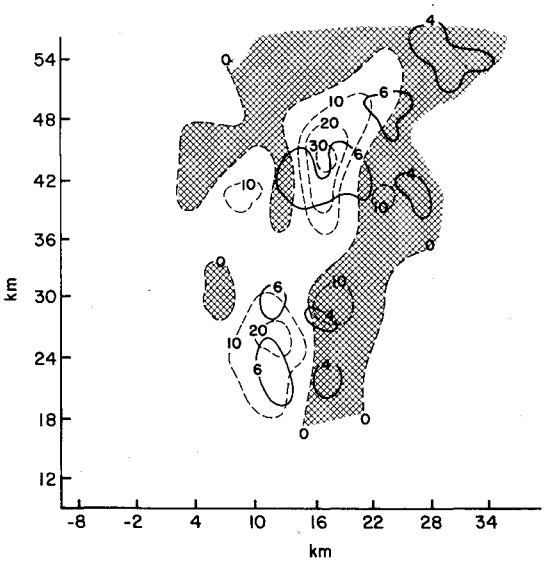

Fig. 5 June 8, 1974: Spectrum width (m s^{-1}) contours are solid lines; vertical motion (m s^{-1}) contours are dashed lines. Cross-hatched area is downdraft. The origin of the coordinate system is at the radar site.

Using the new display for planning, we directed a number of thunderstorm penetrations by an Aeronautical System Command F-4-C aircraft, and were successful in locating areas where the aircraft experienced turbulence. The data were searched for significant correlations. That between turbulence and radar echo intensity remained essentially as observed in the mid-1960 program—that is, turbulence moderate or greater can be expected somewhere in a storm when the maximum reflectivity factor of the storm is 40 dBZ or more.[14] In addition to reflectivity, a number of other radar associated parameters were considered. A typical time-history of these parameters is shown in Fig. 3.

Note how well the turbulence trend matches the trend in the spectrum width plot. A total of 45 penetrations were analyzed, and all evidenced a similar relationship. During these 45 penetrations there were 76 occurrences of moderate or larger turbulence. Ninety-five percent had spectrum widths of 4.0 m s^{-1} or more.[16] In analyzing two of the cases when the spectrum width was less than 4 m s^{-1} but the recorded derived gust velocity exceeded 6.1 m s^{-1}, it appears from the recorded aircraft elevator deflection that the derived gust velocity values were influenced by pilot input (i.e., some component of the pilot-induced vertical acceleration).

In a more recent experiment (June 1980), a NASA F-106 jet aircraft made several penetrations through thunderstorms. On June 16 the aircraft encountered moderate-to-severe turbulence over a sizable portion of one penetration. A point-by-point comparison of spectrum width with the departure of vertical aircraft acceleration from the one due to gravity is shown in Fig. 4. Spectrum width values are either maxima over 1-km flight paths or averages over such paths. The widths are from radar resolution volumes that contained the aircraft path and owing to its constant altitude two elevation angles were used for obtaining Fig. 4. Accelerations are maximum deviations from 1 *g* over a 10-s interval. Again, the turbulence plot matches quite well the spectrum width, considering that up to 2 min of time difference existed between the aircraft measurement and the radar records at the plane altitudes. Corrections due to storm motion over such time differential have been incorporated in the analysis.

The spectrum width may itself at times be biased by wind shear and beam broadening (see Sec. V B). This means that there are some nonturbulent areas where the spectral width is large. However, in three tornadic storms studied, the cumulative probability for spectrum width 4 m s^{-1} or more due to all factors is only about 30%.[5] For nonsevere storms

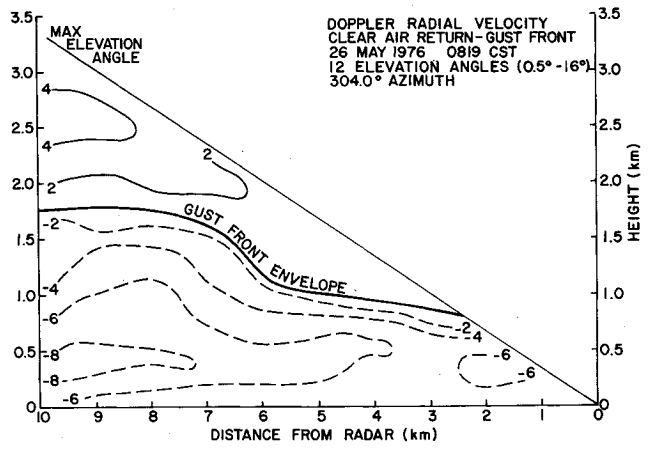

Fig. 6 Clear air single Doppler wind cross section of gust front along 304.0-deg radial, May 26, 1976. Positive (away from radar) isotachs (m s $^{-1}$) are solid, negative isotachs, dashed.

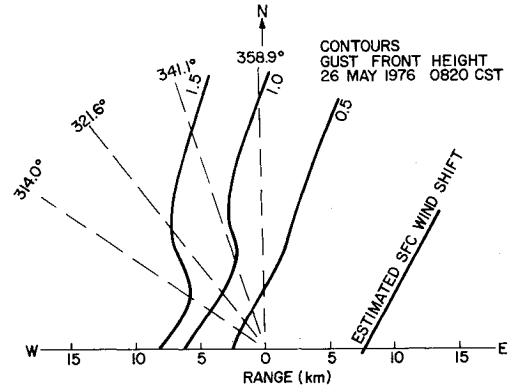

Fig. 7 Height contours of gust front as determined from vertical cross sections obtained from Doppler radar, May 26, 1976, 0820 CST.

the probability is even less, thus only a small portion of even a severe storm could have an "overforecast" condition.

The other parameters investigated were not as promising and when quantities involving shear alone are used, its dependence on viewing angle (tangential shear cannot be determined with a single Doppler radar) would appear to reduce shear's operational utility. Turbulence due to convective processes is less dependent on viewing angle.

Insufficient Doppler data are available for final conclusions concerning locations of broad Doppler spectra in a storm. However, Fig. 5 is presented to show probable correlation between turbulence and the up- (down-) drafts in a tornadic storm. We show here only a 5-km-height section. The maximum reflectivity (not shown) is north of the updrafts. It is apparent in this case that areas of large spectrum broadness are on the edges of the updraft with a preference for higher values when a downdraft is in close proximity. Thus, in this example, turbulence is most probably produced by horizontal shear of the vertical wind.

B. Gust Front and Wind Shear Detection

1. Single Doppler

It has been demonstrated[17] that moderately sensitive Doppler radars can detect motions of air that are void of hydrometeors. Echoes are due to the fluctuation of the refractive index on scale sizes that equal one-half of the radar wavelength. Fluctuations are strongest in the planetary boundary layer and are detectable practically all the time.[18] Thus investigations were started on detection probabilities for gust fronts, wind shear, and other transient hazards from thunderstorms near airports.

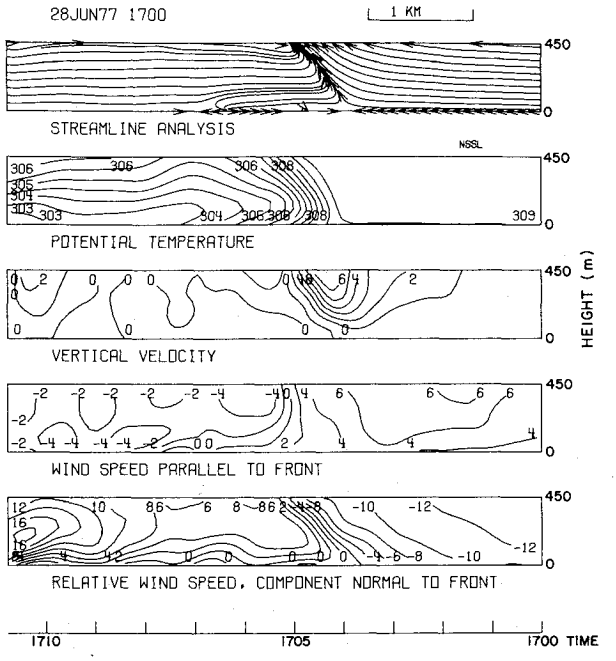

Fig. 8 Gust front time-height cross sections, June 28, 1977, as recorded at the KTVY-TV tower (similar to Fig. 7).

The first observations of a clear air gust front by a Doppler radar occurred on May 26, 1976. Data were obtained from 8 to 12 elevation angles scanned at selected azimuths. Recording started at 0819, or 20 min after the windshift, but 30 min before rain reached Norman. Data were abstracted at 1-km intervals along each elevation angle, analyzed, and cross sections (Fig. 6) produced. Negative numbers indicate motion toward the radar.

Note that the radar is in the cold air; the scans are toward the northwest; and the winds of 8 m s $^{-1}$ at 400 m are slightly less than recorded at the tower, probably because of smoothing effects of the radar resolution volume. The top of the gust front (cold air outflow), chosen as the layer where the radial component reverses sign, is plotted on a polar diagram and height contours drawn (Fig. 7). The outflow frontal slope in the lower boundary layer is about 40 deg. Thus, as the cold air depth increased to 1 km, the slope decreased to 11 deg and continued to flatten out from there to the 1.8-km outflow depth.

Another gust front situation is shown in Fig. 8, a time-height cross section of a gust front passage at the KTVY-TV tower on June 12, 1977, and in Fig. 9, the real-time Doppler radar display at a corresponding time. Surface gusts at the tower reached 28 m s $^{-1}$ after passage of the gust frontal boundary. A sharp temperature discontinuity is evident across the front as the temperature dropped about 6°C in 5 min. Pregust front updrafts are greater than 6 m s $^{-1}$. The Norman Doppler real-time display (Fig. 9) at 1642 CST is taken when the squall line leading edge is about 10 km away from the tower. The reflectivity pattern is typical with weaker values along the edge of the squall line and with numerous embedded cores. Central core values are greater than 40 dBZ. The velocity display shows clear evidence of strong outflow winds ($\pm$32 m s $^{-1}$ toward the radar) along the forward edge of the line. These velocity maxima are displaced from the reflectivity cores by an appreciable amount. From the reflectivity display alone, one may have judged the center portion of the squall line to be weaker than the extremities. The Doppler velocity display, however, shows this area having strong winds (gust front). This is an excellent example of how Doppler radar can detect outflow winds. Damage from this squall line was confined to disruption of electric power distribution system caused by wind and lightning.

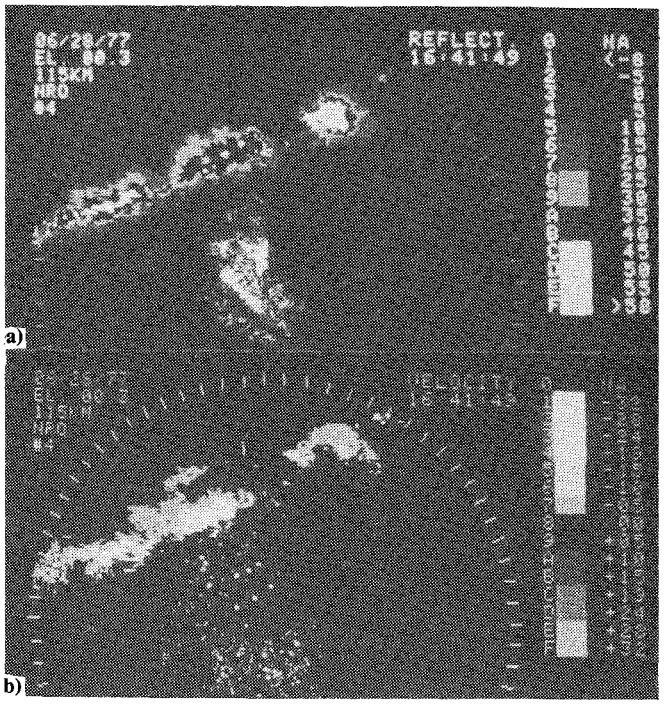

Fig. 9 June 28, 1977, real-time Doppler radar display of a) radar reflectivity pattern with reflectivity factor (dBZ) scale given at right, and b) Doppler radial velocity with velocity scale (m s^{-1}) at right. Range marks for a and b: 40 km. Elevation angle is 0 deg.

C. Glide Slope Experiment

In the spring of 1979, the NSSL's Doppler radar took part in an auxiliary experiment of the SESAME 1979 program.[19] Radar-measured radial velocities along a 3-deg glide path were compared to the longitudinal velocities (parallel to the aircraft axis) recorded by a Queen Air aircraft from the National Center for Atmospheric Research (NCAR). Contiguous time series data spaced 150 m were collected typically from 3.5 to 22.5 km. Simultaneous display of 16 spectra was used to track the aircraft in real time and to derive later on the mean Doppler velocities of clear air echoes.

Two types of aircraft and Doppler wind measurements were performed. In one, termed Lagrangian (Fig. 10), the aircraft velocities were compared with the radar measured winds immediately ahead of the aircraft. A second measurement we call Eulerian because it was an instantaneous picture of velocity distribution along the flight path. One sample was collected immediately prior to the flight and the other immediately after. This allowed not only comparison with the Lagrangian measurement, but also an assessment of the coherency of the wind field over the approximately 4 min it took for an approach.

Altogether 12 approaches were analyzed and in 75% of the cases the aircraft derived velocities agreed well with the radar measurement. Furthermore, the coherency of the field was very good, i.e., there was little difference between the Eulerian measurements before and after the approach and the Lagrangian velocities. Some advection of turbulent features were usually evident from the two Eulerian data.

Somewhat disturbing was the fact that 25% of the approaches did not bear resemblance to radar measured winds. Part of the discrepancy is due to the fact the aircraft path and the radar beam could not be precisely colocated but were offset about a kilometer. Also, the radar measurements are resolution volume weighted while the aircraft senses point velocities. The biggest problem seems to have been moving point targets through sidelobes, and these can be reduced by proper antenna shrouding.

In summary, the glide slope experiment confirmed that a pulsed Doppler radar can monitor wind in clear air along an aircraft approach path. It became evident that the lifetimes of turbulent features in a lightly perturbed planetary boundary layer are well over 4 min. Further experiments are needed to ascertain the transient behavior of the atmosphere in the vicinity of thunderstorms.

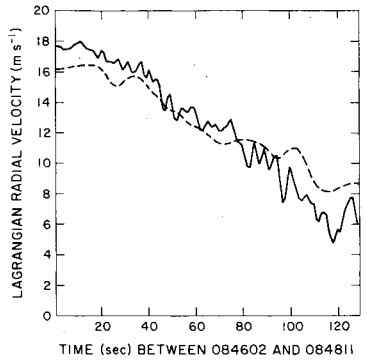

Fig. 10 Aircraft measured longitudinal winds along flight path are depicted with a solid line; the dashed line shows the Doppler measured winds at the first clear gate ahead of the aircraft. The aircraft speed was about 60 m s^{-1} so that 10 s corresponds to 60 m (from 19).

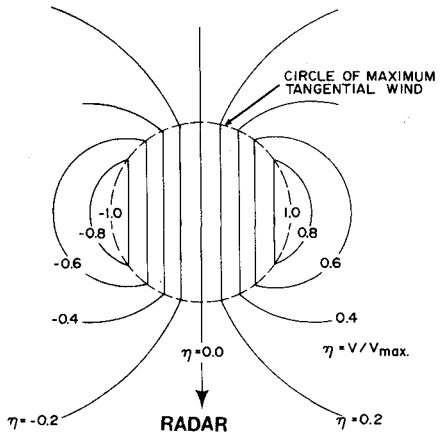

Fig. 11 Simulated single Doppler velocity pattern of a stationary cyclonic vortex.

A simulation study by Strauch and Sweezy[20] showed that the Doppler radar can serve the following functions: 1) It can measure vertical profiles of horizontal wind to 500 m altitude or more even if the wind field varies with altitude and varies linearly with horizontal distance. 2) It can measure the head winds along approach and departure paths whenever the radar is located, such that the aircraft path is approximately towards or away from the radar. 3) If the radar is not suitably located to measure head winds along the aircraft track, the radar can measure the radial profile along the approach path and check if it is consistent with the vertical profile of horizontal wind.

D. Atmospheric Vortices

If a Doppler radar were to scan across a stationary nondivergent mesoscale cyclonic circulation having the tangential velocity distribution of a Rankine combined vortex—that is, velocity increases linearly with radius until a maximum velocity is reached then decreases inversely proportional with radius—a characteristic mean Doppler velocity pattern would result (Fig. 11). Tangential flow perpendicular to the radar beam produces zero Doppler velocity along a radial line from the radar through the center of the circulation. Closed isopleths of maximum Doppler velocities occur at the radius of maximum velocity where the radar beam is parallel to the tangential flow. Presence of divergence (convergence) rotates the pattern counterclockwise (clockwise) relative to the radial line from the radar to the circulation center.

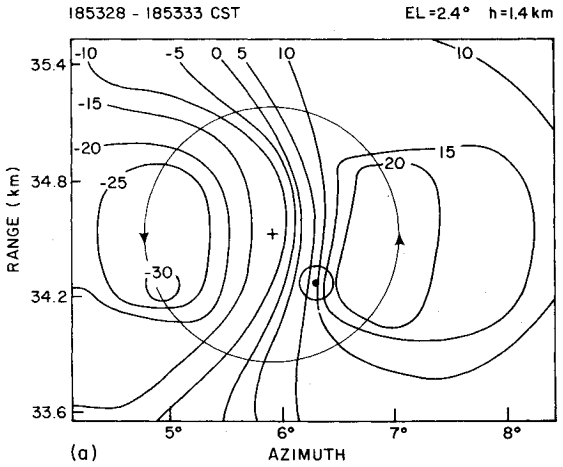

Fig. 12 Radial velocity field of a mesocyclone in m s^{-1} obtained with a single Doppler radar. Data spacing in azimuth is at 0.2 deg and in range at 600 m; height above ground is 1.4 km. The mesocyclone center is indicated with a +; the small circle southeast of it is the tornado to scale. Range and azimuths are with respect to Norman, Okla.

Donaldson[21] has set forth criteria for distinguishing a mesoscale cyclone from a region of cyclonic shear. Briefly, he stipulates that the Doppler velocity shear pattern should remain sufficiently steady during the time required for half a revolution, that its vertical extent be greater than its diameter (distance between peak velocities), and that the pattern remain essentially unchanged as a function of azimuth from the radar. These criteria are satisfied for the mesocyclone signature shown in Fig. 12. This mesocyclone occurred on May 20, 1977 in Del City, Oklahoma. It produced several tornadoes that did some damage to the city. Based on measurements in severe Oklahoma storms, typical mesoscale cyclones have maximum Doppler velocities ranging from 15 to 30 m s^{-1} with peak-to-peak (wind) diameters of 5-10 km (circulation diameters of 10-25 km).

Data confirm mesocyclones to be an excellent severe storm warning criterion. Severe weather (tornadoes, wind, or hail) occurred with 96% of mesocyclones and 50% produced tornadoes. Near severe weather production time, mesocyclones averaged 4.7 km in diameter, rotated at 20 m s^{-1}, and had horizontal cyclonic shear of 1×10^{-2} s^{-1}.

Wind advisories are very important to protection of aircraft and operation on Air Force bases. Advisories were prepared for surface wind (associated with convection) greater than 50 knots (W2) and between 35 and 50 knots (W1). Owing to the difficulty in discerning a signature for the wind case, the Doppler team issued advisories based only on radial velocity magnitudes observed near the ground. High winds perpendicular to the radar beam yielded small radial velocity and a failure to detect.

VI. Summary

The introduction of Doppler capability into weather radars has opened new avenues for both en route and terminal applications. The success achieved with these radars in detection of cyclonic circulations in thunderstorms well in advance of low level intensification (tornado formation) should cause incorporation of coherent systems in new radars used for operation by the national services. Advances in digital processing and display techniques have allowed economical presentation in real time of the three principal Doppler spectral moments.

It is extremely important to relate widths to severe turbulence so that radars can give reliable measure of turbulence hazardous to aircraft. Experiments at the National Severe Storms Laboratory (NSSL) suggest a strong connection between spectral width and aircraft penetration measurements of turbulence. Data show when aircraft-derived gust velocities exceed 6 m s^{-1}, corresponding to moderate or severe turbulence, that the spectral width exceeds 5 m s^{-1} in every case for aircraft within 1 km of the radar resolution volume. Not all storm regions of large spectral width produce aircraft turbulence. Furthermore, when σ_v was less than 4 m s^{-1}, the aircraft experienced only light turbulence in over 50 thunderstorm penetration flights. Accurate estimates of turbulence and shear, as well as rain and hail hazards, should allow safer flights through showers produced by thunderstorms.

Preliminary results on gust front measurements show that a single Doppler radar can successfully track the frontal discontinuity of velocities and thus map the front itself. Because coherent processing improves detection performance by an order of magnitude, shear and turbulence can be measured along the glide slope and around the terminal area even when echoes are due to refractive index fluctuations of clear air.

Acknowledgments

The authors are indebted to the many who assisted in the data collection and analysis and in the preparation of this paper. In particular, we would like to thank Ms. Joy Walton for the typing. Dr. John McCarthy, NCAR, graciously provided Fig. 11 from his experiments during Spring 1979. We also want to acknowledge support by the FAA under Contracts DRFA 01-80-Y-10524 and FA77WAI-808 and the Nuclear Regulatory Commission under Contract NRC AT(49-25)-1004 under which a portion of the work was accomplished and to NASA Langley Research Center for their support of the F-106 aircraft.

References

[1] Doviak, R. J., Sirmans, D., Zrnic', D., and Walker, G.B., "Considerations for Pulse-Doppler Radar Observations of Severe Thunderstorms," *Journal of Applied Meteorology,* Vol. 17, Feb. 1978, pp. 189-205.

[2] Atlas, D., "Advances in Radar Meteorology," *Advances in Geophysics,* edited by H.E. Landsberg and J. Van Mieghem, Academic Press, New York, 1964, pp. 317-478.

[3] Zrnic', D., "Spectral Moment Estimates from Correlated Pulse Pairs," *IEEE Transactions on Electronic Systems,* Vol. AES-13, April 1977, pp. 344-354.

[4] Lee, J.T., "Potential Use of Doppler Weather Radar for Real-Time Warning of Weather Hazardous to Aircraft," *Safe Journal,* Vol. 9, Summer Quarter 1979, pp. 7-10.

[5] Doviak, R.J., Zrnic', D.S., and Sirmans, D.S., "Doppler Weather Radar," *Proceedings of IEEE,* Vol. 67, 1979, pp. 1522-1553.

[6] Lhermitte, R.M., "Motions of Scatterers and the Variance of the Mean Intensity of Weather Radar Signals," Sperry-Rand Research Center, 5RRC-RR-63-57, Sudbury, Mass., 1963.

[7] Nathanson, F.E., *Radar Design Principles,* McGraw-Hill Book Co., New York, 1969.

[8] Frisch, A.S. and Clifford, S.F., "A Study of Convection Capped by a Stable Layer Using Doppler Radar and Acoustic Echo Sounders," *Journal of Atmospheric Science,* Vol. 31, Sept. 1974, pp. 1622-1628.

[9] Frisch, A.S. and Strauch, R.G., "Doppler Radar Measurements of Turbulent Kinetic Energy Dissipation Rates in a Northeastern Colorado Storm," *Journal of Applied Meteorology,* Vol. 15, Sept. 1976, pp. 1012-1017.

[10] Lee, J.T., "Thunderstorm Turbulence—Concurrent Doppler Radar and Aircraft Observations 1973," *Preprints, 6th Conference on Aerospace and Aeronautical Meteorology,* American Meteorological Society, Boston, Mass., 1974, pp. 295-298.

[11] Houbolt, J.C., Steiner, R., and Pratt, K., "Dynamic Response of Airplanes to Atmospheric Turbulence Including Flight Data on Input and Response," NASA TR R-199, June 1964, pp. 7-18.

[12] Ashburn, E.V., Waco, P.E., and Melvin, C.A., "High Altitude Gust Criteria for Aircraft Design," Air Force, Flight Dynamics Laboratory, AFFDL-TR-70-101, Oct. 1970.

[13] Armstrong, G.M. and Donaldson, R.J. Jr., "Plan Shear Indicator for Real-Time Doppler Radar Identification of Hazardous Storm Winds," *Journal of Applied Meteorology,* Vol. 8, June 1969, pp. 376-383.

[14] Burnham, J. and Lee, J.T., "Thunderstorm Turbulence and Its Relationship to Weather Radar Echoes," *Journal of Aircraft,* Vol. 6, Sept. 1969, pp. 438-445.

[15] Burgess, D.W., Hennington, L., Doviak, R.J., and Ray, P.S., "Multimoment Doppler Display for Severe Storm Identification," *Journal of Applied Meteorology,* Vol. 15, Dec. 1976, pp. 1302-1306.

[16] Lee, J.T., "Applications of Doppler Weather Radar to Turbulence Measurements Which Affect Aircraft," FAA Rept., FAA-TF-77-145, March 1977.

[17] Hennington, L., Doviak, R.J., Sirmans, D., Zrnic′, D., and Strauch, R.G., "Measurements of Winds in the Optically Clear Air With Microwave Pulse-Doppler Radar," *Preprints, 17th Conference on Radar Meteorology,* American Meteorological Society, Boston, Mass., Oct. 1976, pp. 342-348.

[18] Chadwick, R.B., Moran, K.P., Morrison, G.E., and Campbell, W.C., "Measurements Showing the Feasibility for Radar Detection of Hazardous Wind Shear at Airports," Final Rept., AFGL Technical Report AFGL-TR-78-0160, 1978.

[19] McCarthy, J., Elmore, K.L., Doviak, R.J., and Zrnic′, D.S., "Instrumented Aircraft Verification of Clear-Air Radar Detection of Low-Level Wind Shear," *Preprints, 19th Conference on Radar Meteorology,* American Meteorological Society., Boston, Mass., April 1980, pp. 143-149.

[20] Strauch, R.G. and Sweezy, W.B., "Wind Shear Detection with Pulse Doppler Radar," Wave Propagation Laboratory, NOAA Final Rept., FAA-RD-80-26, prepared for U.S. Dept. of Transportation, 1980.

[21] Donaldson, R.J. Jr., "Vortex Signature Recognition by a Doppler Radar," *Journal of Applied Meteorology,* Vol. 9, Aug. 1970, pp. 661-670.